

---

10.	<b>TOWARDS A SUSTAINABLE FUTURE: INSIGHTS INTO RENEWABLE AND NONRENEWABLE ENERGY</b> Rohit Kumar, Jitendra Pal Singh and Ashok Kumar	88 – 103
11.	<b>EXPLORING GENERATIVE AI AND COMPUTATIONAL INTELLIGENCE FOR BREAST CANCER DETECTION: A HYBRID APPROACH</b> J. Jebathangam and K. Kasturi	104 – 124
12.	<b>SYNTHESIS OF SILVER NANO PARTICLES</b> Rishu, Rajender Kumar Gupta, Vijeta and Priyanka Joshi	125 – 135
13.	<b>THE CHEMISTRY OF ACID RAIN: CAUSES AND ITS IMPACT ON HUMAN AND ENVIRONMENT</b> Poulami Jana and Giridhari Hazra	136 – 145
14.	<b>ADVANCEMENTS AND CHALLENGES IN SPACE FOOD TECHNOLOGY: ENSURING SAFETY, NUTRITION, AND SHELF LIFE FOR ASTRONAUTS</b> Anusha R, Shabna P. T and Noorjahan K	146 – 158

---

## **EXPLORING GENERATIVE AI AND COMPUTATIONAL INTELLIGENCE FOR BREAST CANCER DETECTION: A HYBRID APPROACH**

**J. Jebathangam<sup>1</sup> and K. Kasturi<sup>2</sup>**

<sup>1</sup>Department of Computer Applications (UG),

<sup>2</sup>Department of Applied Computing & Emerging Technologies,

School of Computing Sciences, VISTAS, Chennai, Tamil Nadu

Corresponding author E-mail: [jthangam.scs@vistas.ac.in](mailto:jthangam.scs@vistas.ac.in), [kasturi.scs@vistas.ac.in](mailto:kasturi.scs@vistas.ac.in)

### **Abstract:**

Mammogram is one of the methods in understanding the presence of Microcalcification (MC) in the breast of women. MC is an initial form of breast cancer. With the help of mammogram image, a doctor can understand an approximate amount of MC present in the breast. Many analytical methods have been developed to quantify the amount of MC from the mammogram image. Such analytical methods can help in Computer Aided Detection (CAD) of MC. Commercial software's have been developed to encircle the MC locations. However, there is no guarantee that the information highlighted by the software as MC is real MCs. Many researchers have worked on the implementation of computer aided diagnosis (CAD) of MC. In this research work, the mammogram image is decomposed using wavelet filters. Daubechi wavelet has been used to decompose the given mammogram image into 5 levels. In each level of decomposition, the approximation is further decomposed. Statistical features are calculated from the approximations of each image from each level of decomposition. These statistical features form training patterns and testing patterns of the proposed ANN algorithms. The patterns are used as inputs for the Back-Propagation Algorithm (BPA), echo state neural network algorithm, Fuzzy logic algorithm and Firefly algorithms. Ten mammogram images are used from Mammographic Image Analysis Society (MIAS) database. Two thousand unique patterns are obtained from the 10 images.

From the 2000 patterns, 1000 patterns are used for training the BPA/ESNN/FL/FF. The remaining 1000 patterns are used for testing the BPA / ESNN/FL/FF algorithms. In the training patterns, 500 are with MC and remaining 500 are without MC. In the testing patterns, 500 are with MC and remaining 500 are without MC. Performance of the algorithms is assessed by receiver operating characteristic curve, sensitivity, specificity and accuracy.

The major contribution of the research work is as follows:

1. BPA is combined with wavelets to detect the presence of MC.
2. ESNN is combined with wavelets to detect the presence of MC in mammogram image.
3. The accuracy of FF and ESNN with wavelet in detecting the MC is higher when compared to that of BPA and FL with wavelets.

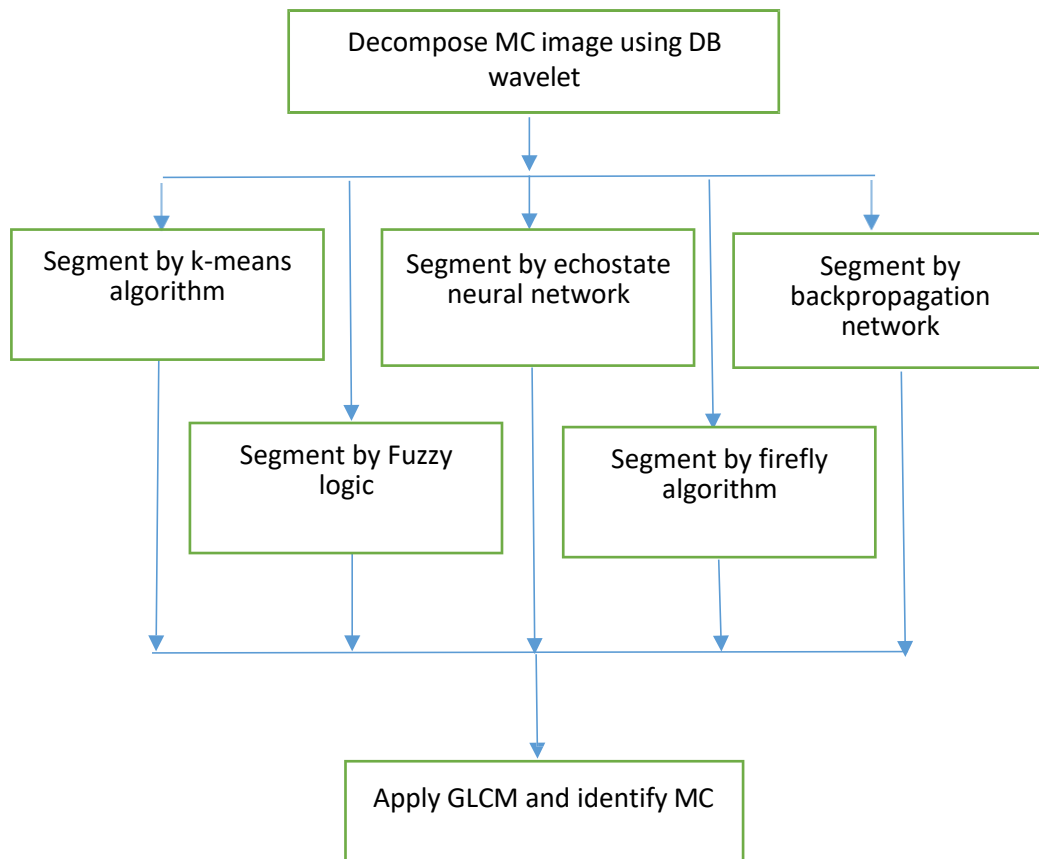
**Introduction:**

Breast cancer is one of the main causes of death in women. Early diagnosis of the human body is an important means to reduce the mortality rate. Mammography is one of the most common techniques for breast cancer diagnosis. Microcalcification (MC) is one among several types of unwanted objects that can be detected in a mammogram. MC is calcium accumulations of 100 microns to several mm in diameter. These are early indicators of the presence of breast cancer. MC clusters are groups of three or more MCs that usually appear in areas smaller than 1cm<sup>2</sup>, with a probability of becoming a malignant lesion.

Calcification in the breast can be seen on a mammogram but cannot be detected by touch. There are two types of breast calcification Macrocalcification and MC. Macrocalcifications are large deposits and are usually not related to cancer. MCs are specks of calcium that may be found in an area of rapidly dividing cells. Many MCs clustered together may be a sign of cancer.

**Problem Statement**

MC is not a regular structure. The density of MC is not uniform with a breast and among different breasts. Identification and quantification of MC to the maximum possible extent in a mammogram breast image is still only an approximate amount of MC quantification. This research work proposes intelligent methods to increase the accuracy of MC quantification.



**Schematic flow for MC identification in breast image**

### **Steps for MC Identification in Breast Image**

1. Input mammogram image.
2. Preprocessing the image.
3. Applying decomposition using wavelets.
4. Obtain statistical features and form a pattern.
5. For each image obtain patterns for training and testing ANN.
6. By using training patterns, store final weights of the ANN at the end of training.
7. During testing process, adopt steps 1-4. Process with the final weights as obtained in step 6.

The outputs of the ANN is used to assess the presence of type of MC.

### **Objectives**

1. To identify the presence of smallest possible MC.
2. To minimize false positive rate and increase the accuracy of the MC identification.

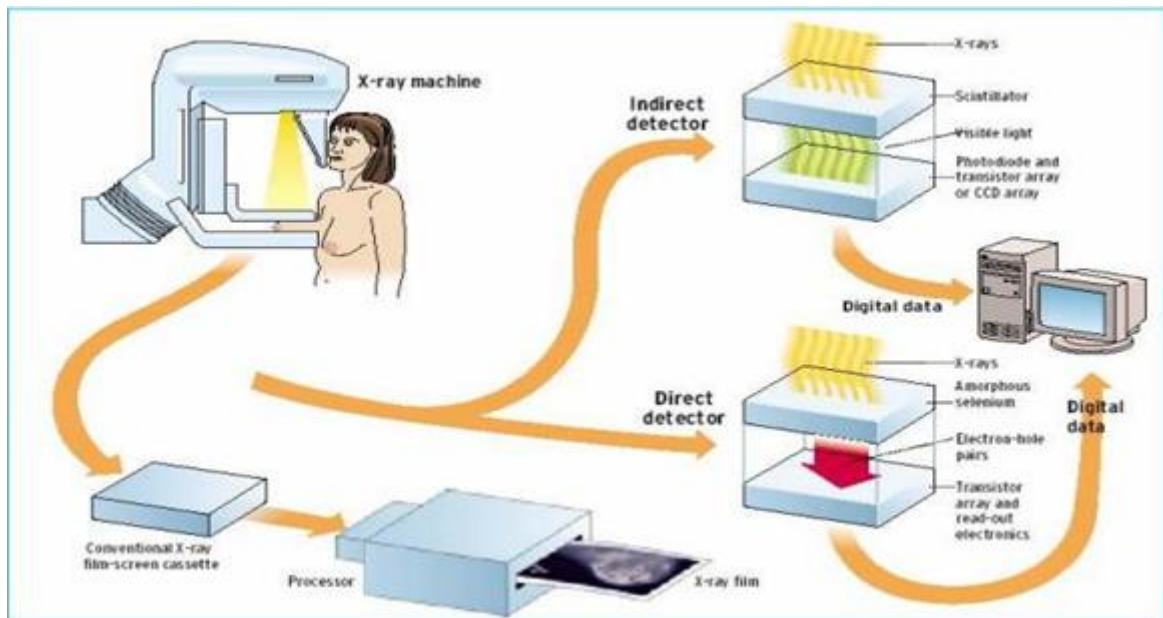
### **Methodologies**

1. Extracting features using Daubechi wavelet.
2. Identify MC using features extracted from Wavelet and with Back propagation algorithm.

3. Identify MC using features extracted from Wavelet and with Echo state Neural Network.
4. Identify MC using features extracted from Wavelet and with Fuzzy Logic algorithm.
5. Identify MC using features extracted from Wavelet and with Firefly algorithm

### Description of Breast Anatomy

A computer system intended for MC detection in mammograms may be based on several methods, like wave lets, fractal models, support vector machines, mathematical morphology, Bayesian image analysis models, high order statistic, and fuzzy logic. Many filters are available for noise reduction in the image. Difference of Gaussian (DoG) fillters is adequate for the noise-invariant and size specific detection of spots, resulting in a DoG image. The use of DoG for detection of potential MCs has been addressed successfully by Osslan Osiris *et al.* (2008).



### Film-Screen and Digital Mammography.

Courtesy: <http://www.spectrum.ieee.org/WEBONLY/pressrelease/0501/cancer0501.pdf>

In all types of mammography, the x-ray photons are given off by the x-ray source and directed towards the patient. In conventional mammography, the development of a film screen cartridge produces the mammogram and is shown in Figure 1.2. In digital mammography, detection can be done in two ways. With indirect detection, x-rays pass through the patient's breast and hit the scintillator. A scintillator is a material that converts x-ray energy into visible light. The scintillator is coupled to a photodetector array or connected to tiles of charge-coupled devices (CCDs) by taped optical fibers. Needle like crystals of cesium iodide (CsI) is typically used as a scintillator. An amorphous silicon

detector made up of photodiodes, and a thin-film transistor (TFT) is used as the readout circuitry. As illustrated in Figure 1.2, with direct detection, the original CCD based indirect system is replaced by amorphous silicon TFT array coated in amorphous selenium. A voltage is placed across the selenium, and wherever an x-ray strikes it, electron-hole pairs are formed. These pairs are then collected by integrated capacitors associated with the pixel elements of the TFT array, and the image is read out by electronics integrated in the array.



### **Digital Mammogram**

Film-screen mammography has saved many lives and it is considered the imaging modality of choice for early detection of breast cancer. Digital mammography provides excellent image quality and has a number of advantages as compared to film-screen mammography systems. Some of these advantages are the potential to acquire the images faster, easily store the images; to manipulate the contrast and magnification of the images, and the potential for digital post processing of the acquired images. One of the limiting problems with conventional mammography is that the recorded image represents the superposition of a three-dimensional (3D) object (i.e., the breast) onto a two-dimensional (2D) plane. Even though breast compression is done, normal anatomical structure can combine with useful diagnostic information (e.g., a tumor mass) in such a way as to impede visualization and reduce lesion detectability.

Breast cancers cause symptoms that tend to be larger, and they may have already spread beyond the breast. In contrast, breast cancers found during the screening process are smaller and they confined to the breast. The size of a breast cancer and how far it has spread are the most important factors in predicting the prognosis (outlook) of a woman with this disease. Most doctors feel that early detection tests for breast cancer can save thousands of lives if more women and their health care providers adopt these tests.

### **Microcalcification**

Existing purpose of mammography is to

1. Early detection of breast cancer, through detection of characteristic masses

2. Detection of MCs.

Existing methods have achieved certain degrees of success in their particular applications. The percentage of FN and FP errors is still too high when using conventional CAD systems. Many solutions have often tended to focus on more sophisticated image processing algorithms for reducing FN and FP errors by providing incremental improvement over existing methods. Thus, there exists a need for an accurate automated method for identifying and assessing clustered structures in a medical image.

Among the characteristics employed by diagnosticians in working with x-ray images of the breast, the following guidelines can be considered:

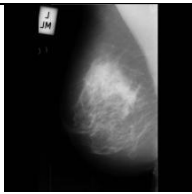
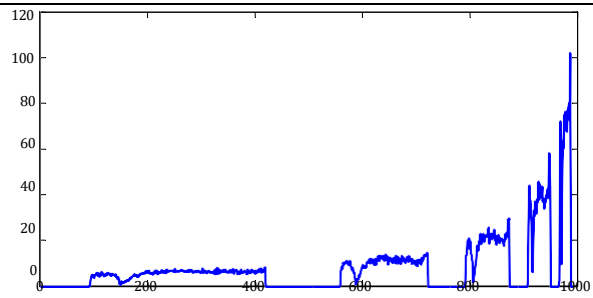
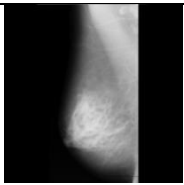
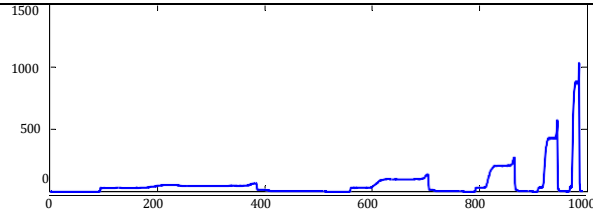
1. Large (>1 mm diameter), coarse calcifications are likely to be benign, but malignant MCs tend to be punctuate, 0.5 mm or smaller;
2. Single calcifications are more likely to be benign;
3. Rounded calcifications of equal size are likely to be benign;
4. Calcifications scattered through both breasts are more likely to be associated with benign disease;
5. Groups of calcifications of mixed size with irregular shapes are more characteristic of malignant than benign condition;
6. Employing these characteristics, Clusters of fine calcifications are more likely to signify malignancy;
7. Rows of fine calcifications within the ducts are likely to signify malignancy
8. Short rods of calcification, particularly if they branch, are highly likely to signify malignancy;
9. Grossly irregular whorled cluster shapes are likely to signify malignancy; and
10. In malignant calcification clusters, the average distance between calcifications is typically less than 1 mm.

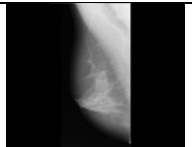
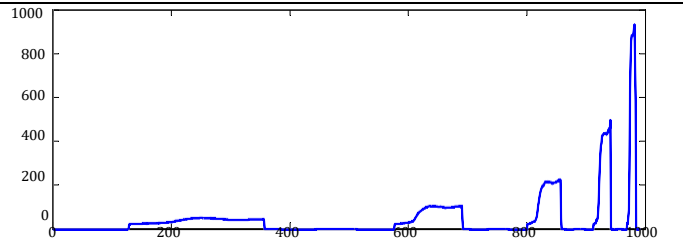
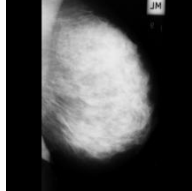
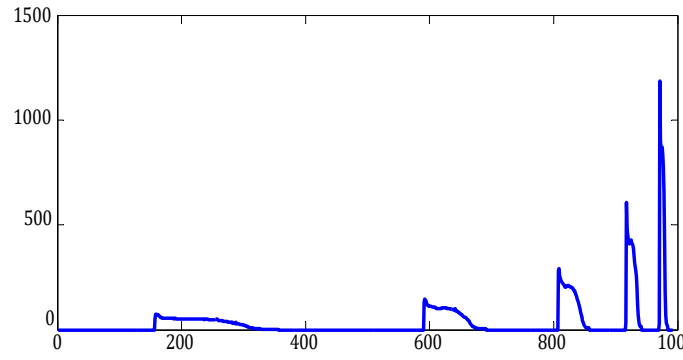
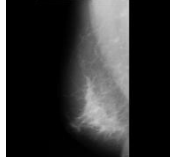
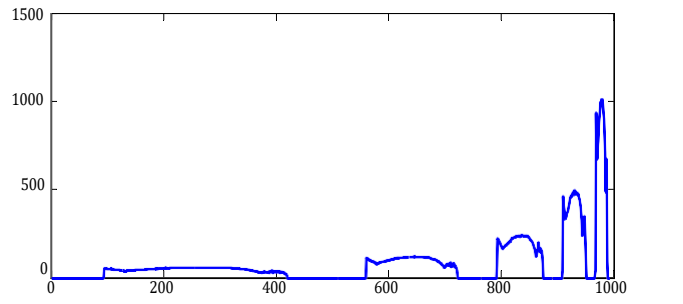
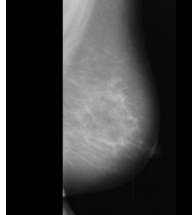
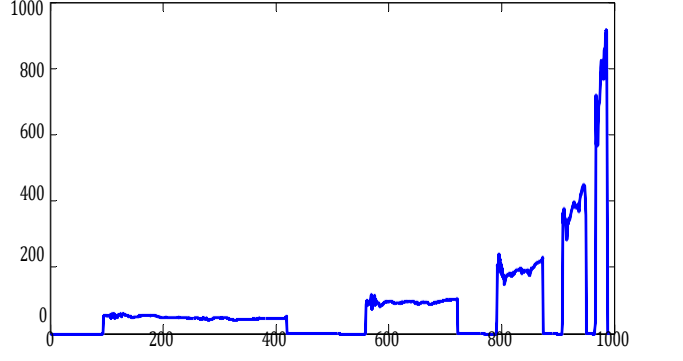
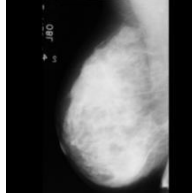
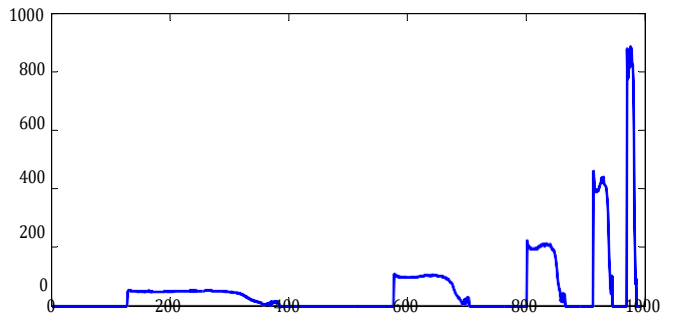
Image analysis methods used in Computer Aided Diagnostics (CAD) systems extract and quantify image data relating to shape, edge character, and intensity at both the spot and cluster level. The shape can be characterized according to its geometric features such as compactness, perimeter, elongation, ratio of moments, and eccentricity. The edge character shows the comparison of the calcification with its background, which can be analyzed by the gradient of the spot boundary and the contrast between the spot and the background. The intensity-based features of the calcification include the mean intensity of a spot as well as the maximum intensity, the deviation of the intensity, the moment, and the like.

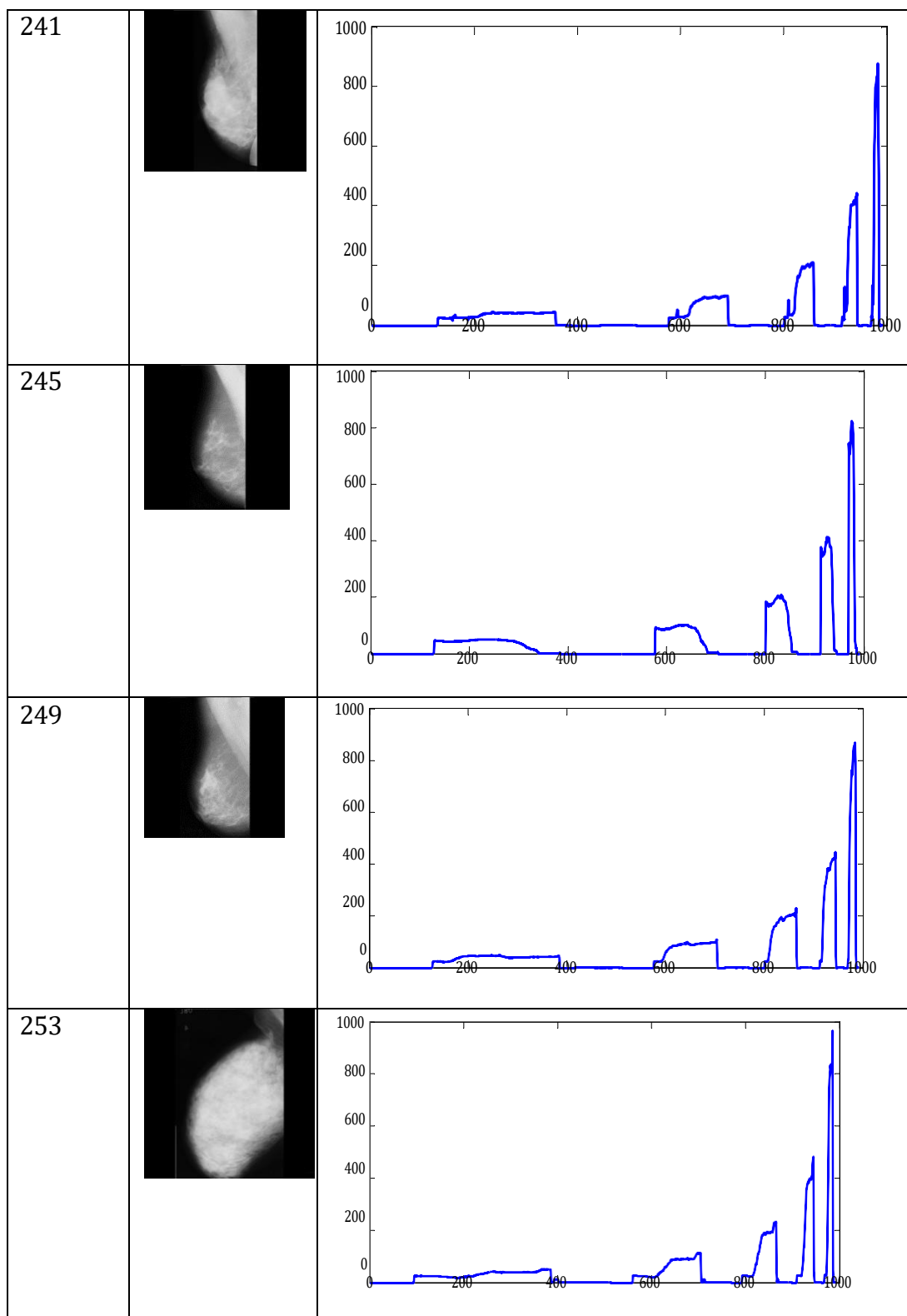
## Image Decomposition Using Wavelets

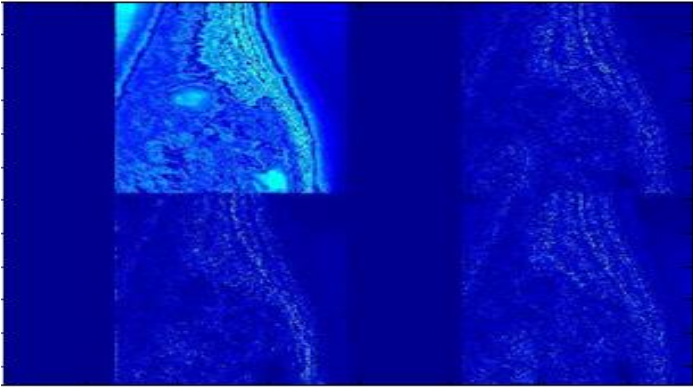
The wavelet (WT) was developed as an alternative to the short time Fourier transform (STFT). A wavelet is a waveform of effectively limited duration that has an average value of zero. Compare wavelets with sine waves, which are the basis of Fourier analysis. Sinusoids do not have limited duration, they extend from minus to plus infinity and where sinusoids are smooth and predictable, wavelets tend to be. Wavelet analysis is the breaking up of a signal into shifted and scaled versions of the original (or mother) wavelet. Mathematically, the process of Fourier analysis is represented by the Fourier transform: which is the sum over all time of the signal  $f(t)$  multiplied by a complex exponential. The results of the transform are the Fourier coefficients, which when multiplied by a sinusoid of frequency, yield the constituent sinusoidal components of the original signal.

The continuous wavelet transform (CWT) is defined as the sum over all time of the signal multiplied by scaled, shifted versions of the wavelet function. The result of the CWT is many wavelets coefficients  $C$ , which are a function of scale and position. Multiplying each coefficient by the appropriately scaled and shifted wavelet yields the constituent wavelets of the original signal.

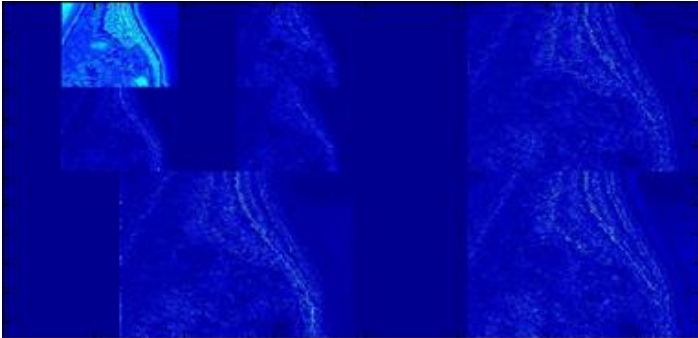
<b>Mammogram and its coefficient</b>		
<b>IMAGE NUMBER</b>	<b>IMAGE</b>	<b>Five level decomposition</b> Each plot, x-label represents five levels of decompositon and y-label represents coefficients
209		
211		

213		
216		
233		
238		
239		





**Level-1 decomposition**



**Level-2 decomposition**

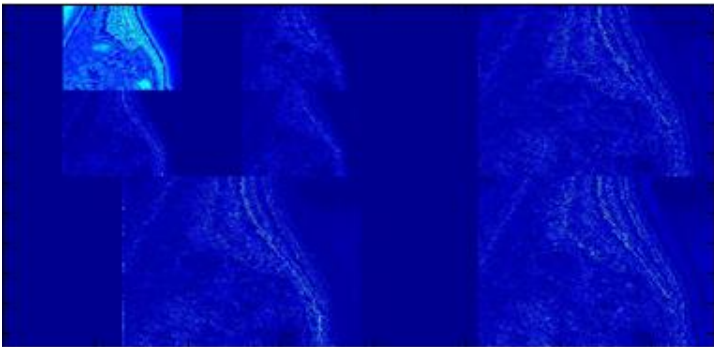
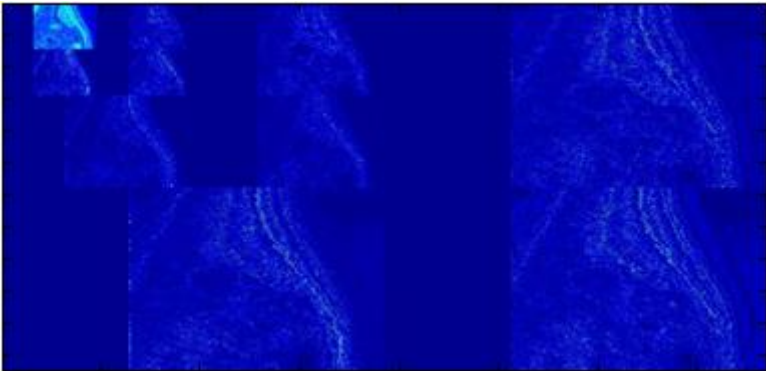
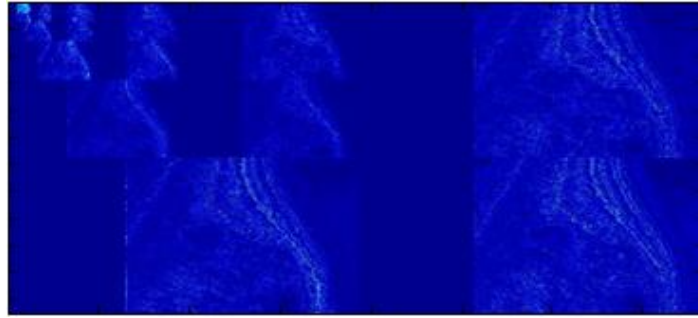


**Fig.3.5 Level-3 decomposition**



**Level-4 decomposition**



**Level-5 decomposition**

### **Artificial Neural Network (ANN)**

An Artificial Neural Network (ANN) is an abstract simulation of a real nervous system that contains a collection of neuron units, communicating with each other via axon connections.

#### **Steps involved in training the BPA Forward Propagation:**

**Step 1:** The weights of the ANN are initialized.

**Step 2:** The inputs and outputs of a training pattern are presented to the network. The output of each node in the successive layers is calculated using equation

$$o(\text{output of a node}) = 1/(1+\exp(-\sum w_{ij} x_i))$$

**Step 3:** The error of a pattern is calculated using equation.

$$E(p) = (1/2) \sum (d(p) - o(p))^2$$

#### **Reverse Propagation (Weight updation)**

**Step 4:** The error for the nodes in the output layer is calculated using equation.

$$(\text{output layer}) = o(1-o)(d-o)$$

**Step 5:** The weights between output layer and hidden layer are updated using equation.

$$W(n+1) = W(n) + \eta(\text{output layer}) o(\text{hidden layer})$$

**Step 6:** The error for the nodes in the hidden layer is calculated

$$\delta(\text{Hidden layer}) = o(1-o) \delta(\text{output layer}) W(\text{updated weights between hidden and output layer})$$

**Step 7:** The weights between hidden layer(s) and input layer are updated using equation.

$$W(n+1) = W(n) + \eta(\text{hidden layer}) o(\text{input layer})$$

The above steps complete one weight updation.

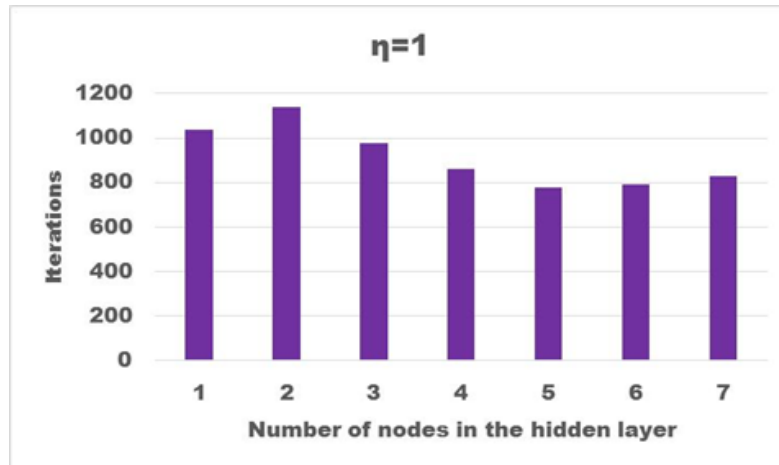
Second pattern is presented and the above steps are followed for the second weight updation. When all the training patterns are presented, a cycle of iteration or epoch is completed. The errors of all the training patterns are calculated using equation.

$$E(\text{MSE}) = \sum E(p)$$

## Results and Discussions:

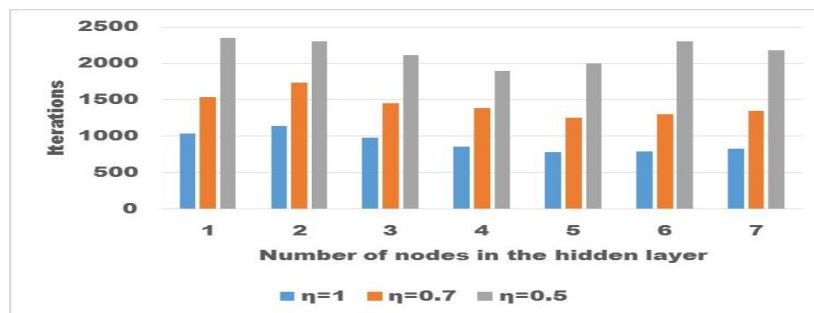
Convergence curve and the percentage of MC detection by BPA

The weight updating algorithm incorporates various parameters to update the weights of the connection strength matrices between input and hidden layer, hidden and output layers. The various parameters used in the BPA algorithms are as follows:  $\alpha$  is an accelerating factor ( $>0$  and  $\leq 1$ )  
 $\eta$  is a learning factor ( $>0$  and  $\leq 1$ )



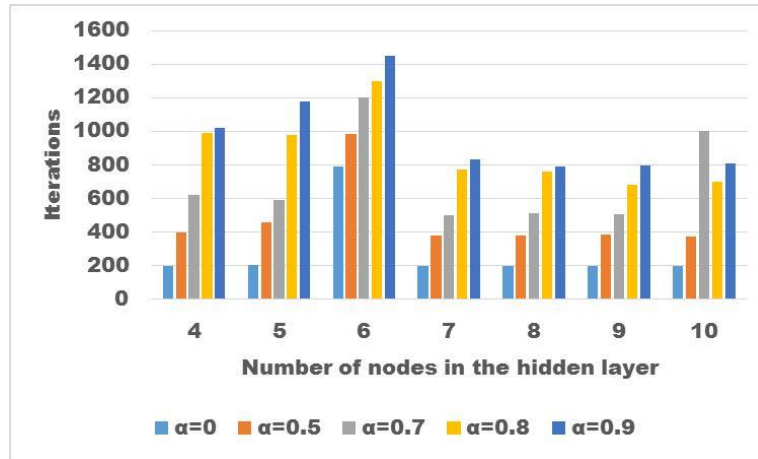
### Effect of number of nodes in the hidden layer for the ANN trained by using BPA

The initialization of the weights and the thresholds are in the range of 0.25 to 0.47. The iterations required by the network which are trained by using BPA for different number of nodes in the hidden layer to reach MSE of 0.01, are shown in Figure 4.4. Number of hidden layer=1 and the =1. X-axis presents number of nodes in one hidden layer.



### Effect of $\eta$ in the ANN trained by using BPA

The learning factor  $\eta$  is supposed to guide the convergence rates of the network to the desired MSE with less number of iterations. It so happens, that sometimes  $\eta$  will make the network to converge to the desired MSE after an increased number of iterations. For 6 nodes in the hidden layer it requires 791 iterations for the network to reach MSE of 0.01 when  $\eta$  is 1.0 and 2300 iterations for the network to reach MSE of when  $\eta$  is 0.05. The convergence rates of the network for various numbers of nodes in one hidden layer for different values of  $\eta$  is shown in Figure 4.5

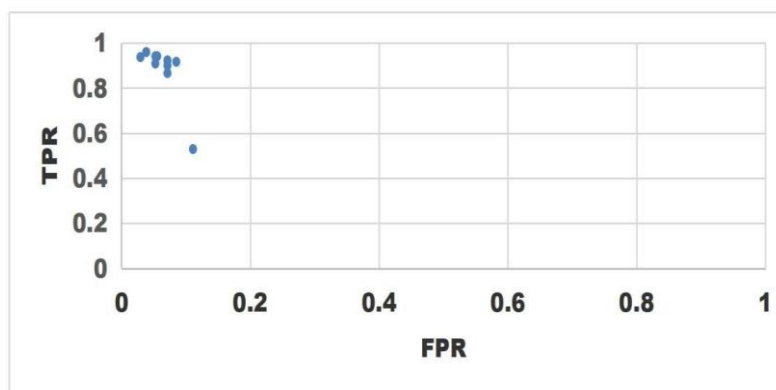


### Receiver Operating Characteristics Curves

ROC is the plot between false positive rate and true positive rate. The points plotted here represent the performance of an algorithm in meeting the expected criteria, it is 90% or above.

When mammogram image is presented to algorithm, how well an algorithm is able to identify the presence of MC to the maximum extent, and how much the algorithm wrongly detects MC. The explanation for TP, TN, FP, and FN are as follows:

1. True positive (TP) - If the pattern contains MC and if the proposed algorithm detects the presence of MC, then it is true positive.
2. False negative (FN)- If the pattern contains MC and if the proposed algorithm does not detect the presence of MC, then it is False negative.
3. True negative (TN): If the pattern does not have MC and if the proposed algorithm does not detect MC, then it is true negative.
4. False positive (FP): If the pattern has no MC and if the proposed algorithm detects the presence of MC, then it is false positive.



**ROC plot for BPA**

The above figure presents the plot for FPR versus TPR. The points obtained are above the diagonal. Hence, the BPA is suitable for detecting MC in mammogram image.

**Echo State Neural Network with Wavelet for Segmentation:**

**Training ESNN**

**Algorithm for Training ESNN**

**Step 1:** Input the features from Wavelet

**Step 2:** Decide the number of reservoirs =21 or 22.

**Step 3:** Decide the number of nodes in the input layer = 5.

**Step 4:** Decide the number of nodes in the output layer = number of target values=1.

**Step 5:** Initialize state vector (number of reservoirs) =0.

**Step 6:** Initialize random weights between input layer (IL) and hidden layer (hL). Initialize weights between output layer (oL) and hidden layer (hL). Initialize weights in the reservoirs.

**Step 7:** Calculate  $state\_vector_{next} = \tanh ((ILhL)weights*Inputpattern + (hL)weights* state\_vector_{present} + (hLoL)weights * Targetpattern)$ .

**Step 8:** Calculate, a = Pseudo inverse (State vector all patterns).

**Step 9:** Calculate,  $W_{out} = a * T$  and store  $W_{out}$  for segmentation.

**Testing ESNN with wavelet**

Algorithm for Testing ESNN or segmenting the image

Testing ESNN (Segmenting image)

**Step 1:** Input the features from wavelet

**Step 2:** Decide the number of reservoirs =21 or 22.

**Step 3:** Calculate state vector =  $\tanh ((ILhL)weights*Inputpattern + (hL)weights* state\_vector_{present} + (hLoL) weights * Target\ pattern)$ .

**Step 4:** Estimated output = state vector \*  $W_{out}$ .

**Step 5:** Assign '0' (black) or '255' (white) in the new matrix which will be the segmented image.

**Segmentation Performance in Terms of Number of Pixels and Number of Objects**

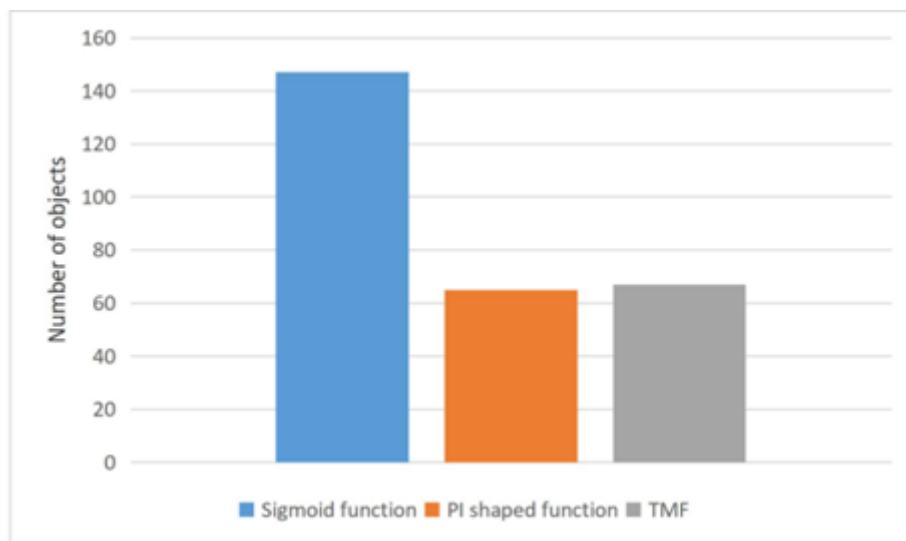
<b>Segmentation Accuracy based on Number of Pixels</b>			
<b>Image</b>	<b>NC</b>	<b>TP (Ground truth)</b>	<b>Apixel (%)</b>
Image 1	344	362	95.01
Image 2	1009	1062	94.99
Image 3	760	792	96.01
Image 4	843	892	94.56
AVERAGE			95.137

### Segmentation Accuracy based on Number of Objects

Image		Solidity	Area	Perimeter	Total	Aprop
Image 1	Segmented	153.8936	227	126.3849	507.2785	
	Unsegmented	170.8582	245	138.3848	554.243	
Image 2	Segmented	132.5644	1439	867.1724	2438.7368	94.93
	Unsegmented	135.5644	1509	924.42	2568.9844	
Image 3	Segmented	170.875	1204	886.2178	2261.0928	96.23
	Unsegmented	175.876	1252	921.7996	2349.6756	
Image 4	Segmented	180.809	979	830.7306	1990.5396	94.32
	Unsegmented	190.701	1039	880.71	2110.4110	
Average:						95.20

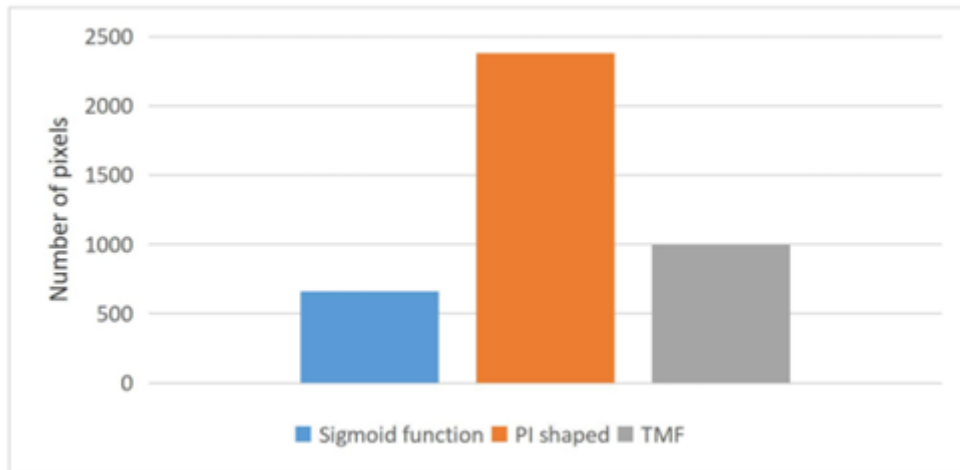
### Fuzzy Logic for Mammogram Segmentation

#### Number of segmented objects and number of segmented pixels



#### Segmented Objects for different membership functions for image-1

The below figure shows the number of objects calculated using region properties of Matlab image-1. The number of objects obtained from segmented images for different membership functions is shown. Optimum number of objects that is 67 is obtained when the triangular membership function is used.



**Segmented Pixels for different membership functions image-1**

### Firefly Algorithm for Segmentation of Mammogram Image

The firefly algorithm (FA), proposed by Xin-She Yang at Cambridge University, is a novel metaheuristic, which is inspired by the behavior of fireflies. Their population is estimated about two thousand firefly species.

FA uses the following three idealized rules:

1. Fireflies are unisex so that one firefly will be attracted to other fireflies regardless of their sex.
2. The attractiveness is proportional to the brightness, and they both decrease as their distance increases. Thus for any two flashing fireflies, the less bright one will move towards the brighter one. If there is no brighter one than a particular firefly, it will move randomly.
3. The brightness of a firefly is determined by the landscape of the objective function. As a firefly's attractiveness is proportional to the light intensity seen by adjacent fireflies, we can now define the variation of attractiveness with the distance  $r$  by equation.

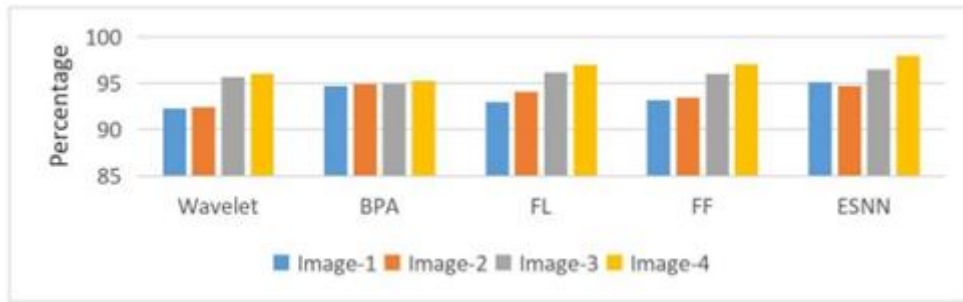
$$r = -2$$

Where  $r$  is attractiveness and  $r=0$ .

The movement of a firefly 'i' is attracted to another more attractive (brighter) firefly 'j' is determined by equation .

$$x_i^{t+1} = x_i^t + r_i^2 (-) +$$

Where the second term is due to the attraction. The third term is randomization with  $r$  being the randomization parameter, and  $\epsilon$  is a vector of random numbers drawn from a Gaussian distribution or uniform distribution at time  $t$ . If, it becomes a simple random walk.



**Segmentation accuracy for wavelet, BPA, FL, FF, ESNN**

### Texture Based Feature Extraction Using Gray Level Co-Occurrence Matrix (GLCM)

For every new occurrence of white pixels and new position of the moving window, the calculation of GLCM features, comparison with the template file, obtaining the lowest Euclidean distance and comparing it with the MC detection threshold is carried out. By adopting the above procedure, the presence or absence of MC in a mammogram can be analysed.

#### Algorithmic steps

**Step 1:** Input black and white images are given from wavelet, BPA, FL, FF and ESNN.

**Step 2:** Locate the white region from the segmented image.

**Step 3:** Correspondingly crop 40 x 40 window in the original image.

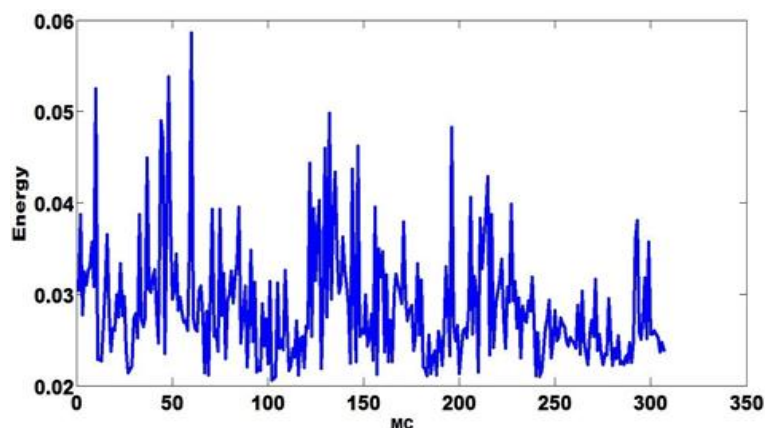
**Step 4:** Calculate the GLCM features such as Energy, Homogeneity, Contrast and Correlation.

**Step 5:** Compare the outputs of step 4 with all rows of MC template file.

**Step 6:** Find the rows in MC template file which is closer to the outputs of step 4 by Euclidean distance.

**Step 7:** If the output of step 7 < Matching threshold, then, a MC is identified

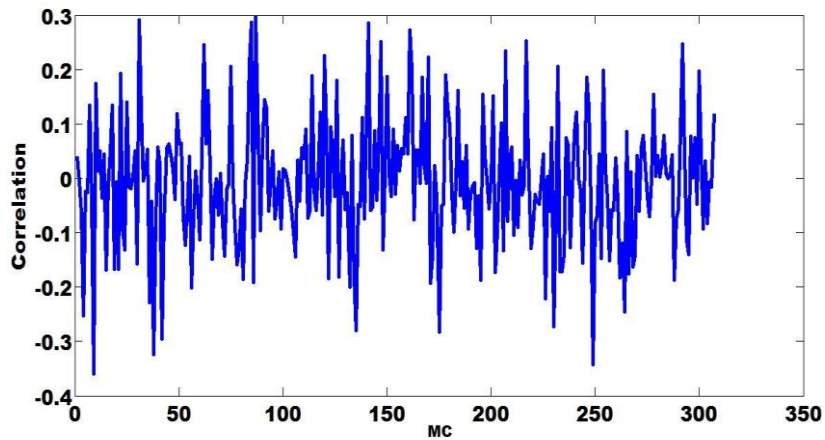
**Step 8:** Go to step 2 until the entire segmented black and white image is covered.



**Energy Values for MC in Different mammogram images**

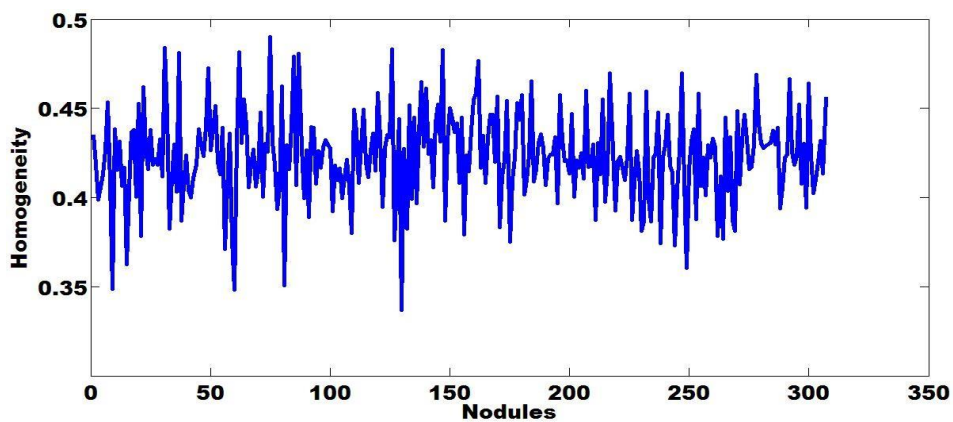
The above figure presents the energy values calculated for MC of different mammogram images. Higher energy values occur when the gray level distribution has a

constant or periodic form. The energy values are in the range of 0.02 till 0.06. It indicates that the MC is represented by a gradual change in its intensity values and it will be useful for the effective identification of different MC.



### Correlation Values for MC in Different mammogram images

The above figure presents the correlation values calculated for MC of different mammogram images. Gray tone linear dependencies in the image are understood by the correlation process. The highest in correlation values indicates more the more similarity in matching. If the correlation is high, then template matching is easier



### Homogeneity Values for MC in Different mammogram images

The above figure presents the homogeneity values calculated for MC of different mammogram images. It has a maximum value when all intensities in the images are same. Since the intensity values are different in the MC, the values of homogeneity are less than 0.5. Hence, MC detection becomes easier.

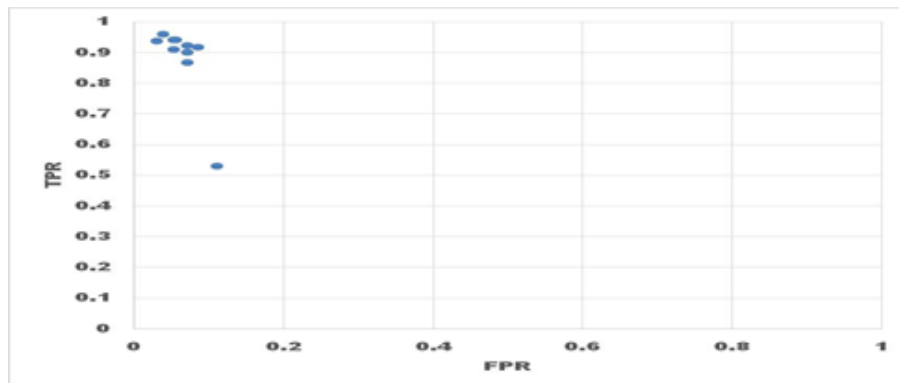
### Performance Comparisons of Segmentation Algorithms

The performance analysis of the proposed MC detection method has been carried out. For this process, images of patients are considered. All the images are segmented by wavelet, BPA, FL, FF and ESNN methods. This MC detection algorithm is applied for all the segmented images obtained from five segmentation algorithms. The algorithm checks the

presence of how many false positive MC are detected in the segmented images which are actually not MC and the number of false negatives are obtained in the images that actually have MC.

To understand the consistency of the proposed algorithm for all the mammograms, a graph is plotted using Receiver operating characteristics (ROC) analysis. The ROC is plotted by calculating the true positive rate and false positive rate. For each mammogram, true positive rate and false positive rate are obtained. Based on the number of mammograms, equal no of points are plotted in the ROC. If the points are found to be above the diagonal, it is an indication of good performance of the proposed MC detection algorithm.

### **ROC Curve**



### **ROC**

The above graph presents the plot for FPR versus TPR. The points obtained are above the diagonal. Hence, the detection of MC by FL is within acceptable region.

### **Conclusions:**

The following outputs are concluded.

- 1) The number of levels of decomposition of mammogram by wavelet affects the microcalcification (MC) identification accuracy.
- 2) The features extracted from the DB wavelet and coiflet wavelet is almost same.
- 3) The Back propagation algorithm takes sufficient number of iterations to learn the coefficients of the decomposed image. The MC identification accuracy depends on the type of input data. BPA should be trained with unique patterns as there will be lot of duplication of the patterns.
- 4) The performance of the FL in identifying the MC depends upon the number of rules used for training the FL.
- 5) To some extent noise is removed during decomposition and reconstruction of the mammogram.

### Future Scope of the Work

The research work implemented in this thesis can be extended to new combinations of algorithms for detecting MC. The new combination can be combining ANN with genetic algorithm, ANN with particle swarm optimization.

### References:

1. AbuBaker, A. (2012). Neuro-fuzzy approach to microcalcification contrast enhancement in digitized mammogram images. *The International Journal of Multimedia & Its Applications*, 4(5), 61–75.
2. AbuBaker, A. (2015). Automatic microcalcification detection using wavelet transform. *International Journal of Computer Theory and Engineering*, 7(1), 40–45.
3. Ahirwar, A., & Jadon, R. S. (2011). Characterization of tumor region using SOM and neuro fuzzy techniques in digital mammography. *International Journal of Computer Science and Information Technology*, 3(1), 199–211.
4. Akila, K., Jayashree, L. S., & Vasuki, A. (2015). Mammographic image enhancement using indirect contrast enhancement techniques—a comparative study. *Procedia Computer Science*, 47, 255–261.
5. Al Mutaz, M. A., Dress, S., & Zaki, N. (2011). Detection of masses in digital mammogram using second order statistics and artificial neural network. *International Journal of Computer Science & Information Technology*, 3(3), 176–186.
6. Alanís-Reyes, E. A., Hernández-Cruz, J. L., Cepeda, J. S., Castro, C., Terashima-Marín, H., & Conant-Pablos, S. E. (2012). Analysis of machine learning techniques applied to the classification of masses and microcalcification clusters in breast cancer computer-aided detection. *Journal of Cancer Therapy*, 3(6), 1020–1028.
7. Alarcon-Aquino, V., Starostenko, O., Ramirez-Cortes, J., Rosas-Romero, R., & Rodriguez-Asmoza, J. (2009). Detection of microcalcifications in digital mammograms using the dual-tree complex wavelet transform. *Journal Title Missing*, 17(1), 49–63.
8. Al-Najdawi, N., Biltawi, M., & Tedmori, S. (2015). Mammogram image visual enhancement, mass segmentation and classification. *Applied Soft Computing*, 35, 175–185.
9. Alolfe, M. A., Youssef, A. M., Kadah, Y. M., & Mohamed, A. S. (2008). Computer-aided diagnostic system based on wavelet analysis for microcalcification detection in digital mammograms. In *Biomedical Engineering Conference, CIBEC, Cairo International* (pp. 1–5). IEEE.

10. Al-Shamlan, H., & El-Zaart, A. (2010). Feature extraction values for breast cancer mammography images. In *Bioinformatics and Biomedical Technology (ICBBT), International Conference on* (pp. 335–340). IEEE.
11. Al-Timemy, A. H., Al-Naima, F. M., & Qaeab, N. H. (2009). Probabilistic neural network for breast biopsy classification. *MASAUM Journal of Computing*, 1(2), 199–205.
12. Anand, S., Vinod, V., & Rampure, A. (2015). Application of fuzzy c-means and neural networks to categorize tumor affected breast MR images. *International Journal of Applied Engineering Research*, 10(64), 274–281.
13. Angayarkanni, P. (2011). MRI mammogram image segmentation using NCut method and genetic algorithm with partial filters. *IJCSI International Journal of Computer Science Issues*, 8(1), 455–459.
14. Antony, S. J. S. (2014). Detected breast cancer on mammographic image classification using fuzzy c-means algorithm. *International Journal of Innovations in Engineering and Technology (IJJET)*, 4(4), 209–215.
15. Arodź, T., Kurdziel, M., Popiela, T. J., Sevre, E. O., & Yuen, D. A. (2006). Detection of clustered microcalcifications in small field digital mammography. *Computer Methods and Programs in Biomedicine*, 81(1), 56–65.
16. Arun, K. S., & Sarath, K. S. (2011). Evaluation of SUSAN filter for the identification of microcalcification. *International Journal of Computer Applications*, 15(3), 41–44.
17. Ashwin, R., Abimannan, T., & Kumar, P. N. (n.d.). Neural network based automatic detection of lesion diagnosis in mammogram using image fusion. *Journal Title Missing*, 2(3), 29–37.
18. Ayer, T., Chen, Q., & Burnside, E. S. (2013). Artificial neural networks in mammography interpretation and diagnostic decision making. *Computational and Mathematical Methods in Medicine*, Article ID 832509, 1–10. <https://doi.org/10.1155/2013/832509>
19. Badawy, S. M., Hefnawy, A. A., Zidan, H. E., & GadAllah, M. T. (2017). Breast cancer detection with mammogram segmentation: A qualitative study. *International Journal of Advanced Computer Science and Applications*, 8(10), 117–120.
20. Bagci, A. M., & Cetin, A. E. (2002). Detection of microcalcifications in mammograms using local maxima and adaptive wavelet transform analysis. *Electronics Letters*, 38(22), 1311–1313.

## SYNTHESIS OF SILVER NANO PARTICLES

Rishu, Rajender Kumar Gupta\*, Vijeta and Priyanka Joshi

Department of Zoology, CCS Haryana Agricultural University, Hisar

\*Corresponding author E-mail: [gupta\\_raj123@yahoo.com](mailto:gupta_raj123@yahoo.com)

### Introduction:

Nano particles are defined as substances measuring between 1 and 100 nanometres in size. In the last decade, a diverse array of nanoparticles (NPs) has seen extensive application worldwide. Numerous studies support the notion that nanotechnology is an expanding commercial field, largely attributed to the increasing variety of products that utilize nanoparticles (Mansoori *et al.*, 2008). The attributes of NPs are driven because of their physicochemical properties, and certain types are produced in significant quantities due to their exceptional qualities (Vali *et al.*, 2022). The discharge of nanoparticles into aquatic habitats occurs at several stages, encompassing their production, usage and the disposal of associated nano-wastes. (Ringwood *et al.*, 2010). In aquatic ecosystems, silver nanoparticles manifest in diverse forms, influenced by water's properties. Water in natural environments moves across land, traversing both surface and subterranean pathways until it arrives at estuarine and subsequently oceanic waters. During this transit, numerous physical transformations occur, which can either reduce the toxicity of the nanoparticles or exacerbate it. If these nanoparticles or their modified versions undergo agglomeration or self-aggregation within biological entities, they may pose serious health risks (Lapresta-Fernandez *et al.*, 2012). Nanoparticles exhibit toxicity that is significantly affected by factors such as their diminutive size, chemical composition, surface morphology, solubility, shape, and their propensity for agglomeration and aggregation. Nonspecific oxidative stress has emerged as a major concern associated with the toxicity induced by nanoparticles. Observations in fish and embryos exposed to these particles reveal various toxicological changes, particularly those related to oxidative stress, including lipid oxidation, programmed cell death (apoptosis), and alterations in gene expression (Mekki *et al.*, 2019). The potential risks posed by nanoparticles (NPs) within aquatic ecosystems can be effectively assessed by examining their bioavailability and toxicity to life which dwells in water (Nowack and Bucheli, 2007). At high concentrations, nano particles and their derivatives which are ionic may engage in interactions that could lead to detrimental effects on organisms which survive in water (Griffitt *et al.*, 2007; Xiang *et al.*,